Numerical Results on Two-Fluid Reconnection and Relaxation with Guide Field

C. R. Sovinec, J. R. King, N. A. Murphy, and V. V. Mirnov

University of Wisconsin-Madison

CEMM Collaboration Meeting

pre-Sherwood

Annapolis Maryland, April 22, 2007

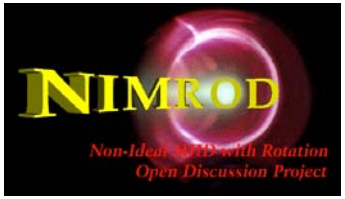

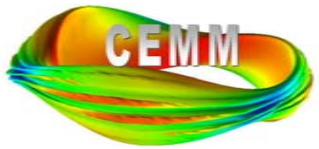

Outline

- Magnetic reconnection
  - Linear, large guide-field computations
  - Scans of equilibrium scale and plasma-β
- Fluid electron stress
- MRX Simulations
- Conclusions

Important properties of linear two-fluid tearing with large guide-field are obtained from sheared slab calculations.

• V. Mirnov, C. Hegna, and S. Prager applied asymptotics to analyze tearing in a wide range of parameters. [Phys. Plasmas **11**, 4481 (2004)]

• In the large guide-field limit, the stability parameter must satisfy

$$\Delta' L \sim \frac{L}{\delta}$$

where L is the equilibrium scale and δ is the reconnection scale to see whistler-mediated effects.

• However, $\rho_s = \frac{c_s}{\Omega_i} = \frac{\sqrt{\beta}}{d_i} > \delta$

allows sound-wave demagnetization (KAW) to increase the tearing rate at small Δ' L.

• Pressure is uniform→no drift effects.

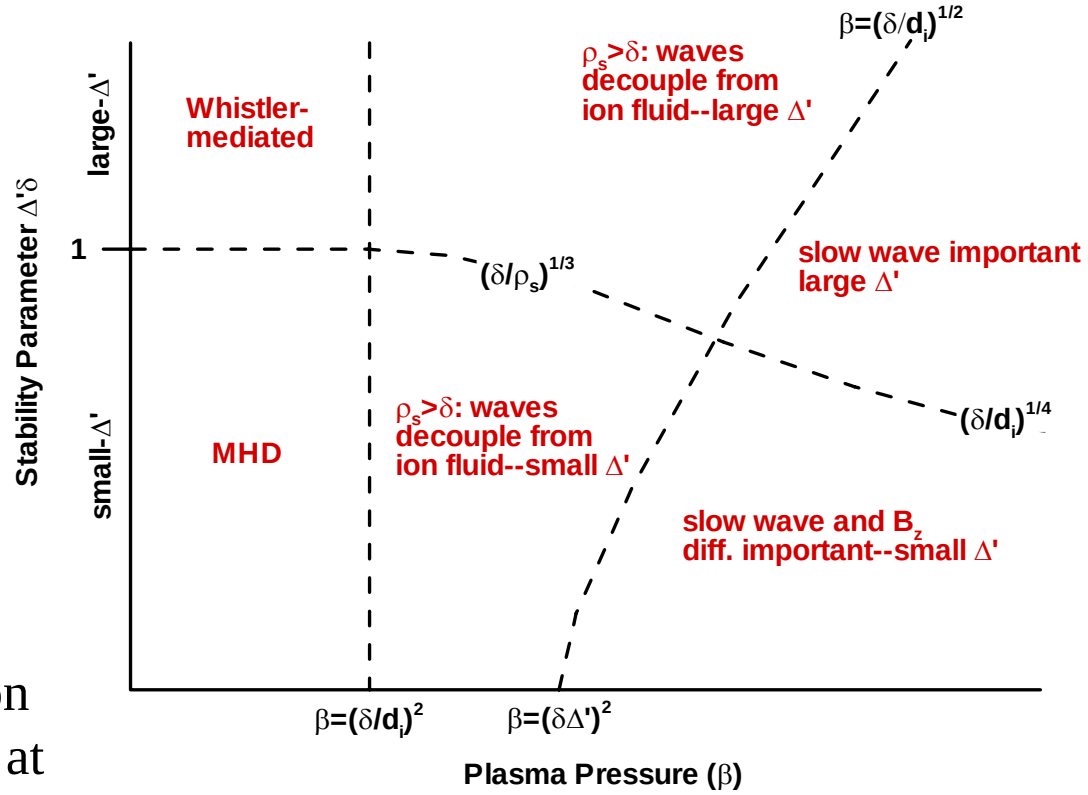

A schematic of the parameter space shows where different effects become important.

Our numerically computed growth rates are in good agreement with the analytical dispersion relation, provided that the tearing layer is sufficiently smaller than the equilibrium scale.

	input					*output*		
CASE	$\Delta' L$	$k\,L$	β	ρ_s / L	$S \equiv \tau_r / \tau_a$	δ / L	$\Gamma \equiv \gamma\,\tau_a / k\rho_s$	Γ_{ana}*
A	0.28	0.93	0.002	0.56	6.7×10^{3}	0.184	8.51×10^{-3}	9.04×10^{-3}
B	0.28	0.93	0.083	3.6	6.7×10^{3}	0.172	1.50×10^{-3}	1.61×10^{-3}
B2	0.28	0.93	0.083	3.6	2.7×10^{4}	0.119	7.77×10^{-4}	8.05×10^{-4}
C	5.3	0.33	0.083	3.6	670	0.11	0.106	0.111
D	5.3	0.33	0.083	3.6	67	0.25	0.203	0.221
E	5.3	0.33	0.083	3.6	6.7	0.65	0.297	0.371
F	24	0.083	0.083	3.6	6.7	1.11	0.401	0.524
G	5.3	0.33	0.83	11.4	6.7	0.48	0.169	0.174

*Computed from the dispersion relation from Mirnov, *et al*.

- The definition of S used here is $S \equiv LB_{y\infty} \Big/ D_\eta \sqrt{\mu_0 \rho}$
- Resistivity is the only dissipation mechanism in Cases A, B, and B2.
- Computations such as Case B are spatially resolved with a 48×6 mesh of bicubic elements, packed such that $\Delta x_0 \sim 0.1\delta \sim 10^{-3} x_{max}$.
- Temporal resolution is achieved at compressional wave-CFL # ~ 10^6.
- The ratio ρ_s/L does not affect the asymptotics.

The computations include five spatial scales: 1) the wall position, 2) the wavelength along the resonance $2\pi/k$, 3) the equilibrium scale L, 4) the sound gyroradius ρ_s, and 5) the reconnection scale δ.

- The NIMROD computations necessarily have boundaries at a finite distance ($>L$) from the tearing layer. Wall locations that do not influence results are determined empirically. $\delta = \sqrt{\eta/\gamma\mu_0}$
- The size of the periodic direction of the slab is used to set k.
- The NIMROD computations have m_e=0, so
  - The scales shown on the parameter-space schematic 'move' for results with different growth rates.

Recent linear computations for the realistic small $\Delta'\delta$ and large β-region consider L larger than ρ_s.

- Parameters for one case are $\Delta' L$=0.277, β=0.083, S=2.7×10^5, a/L=3, ρ_s/L=0.363, δ/L=0.117. [The last is determined by the resulting growth rate.]
- The normalized $\Gamma=8.19\times10^{-4}$ is approximately 1% from the analytical limit of $\Gamma_{(56)}=8.08\times10^{-4}$. [For m_e=0 in this limit, $\Gamma_{(56)}=1.478\Delta'\sqrt{D_\eta\tau_a}/\pi^2 k\rho_s\beta^{1/2}$.]

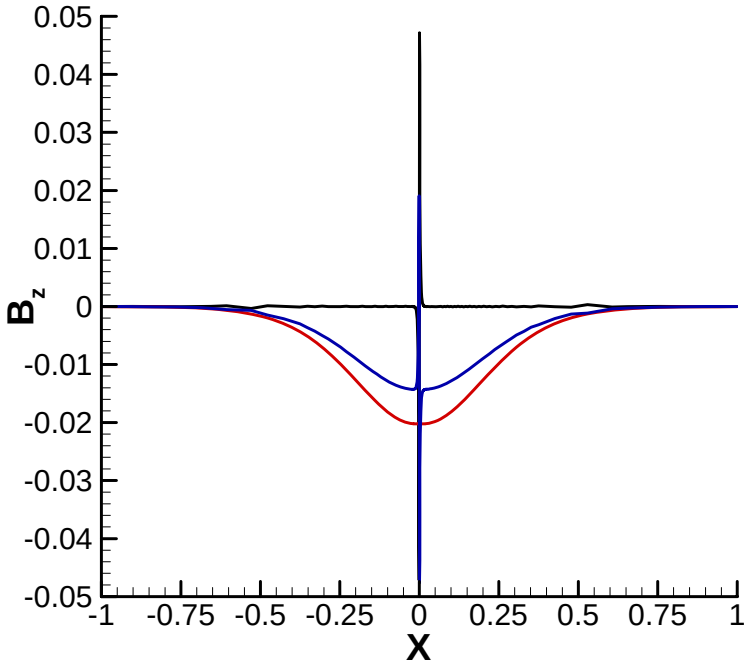

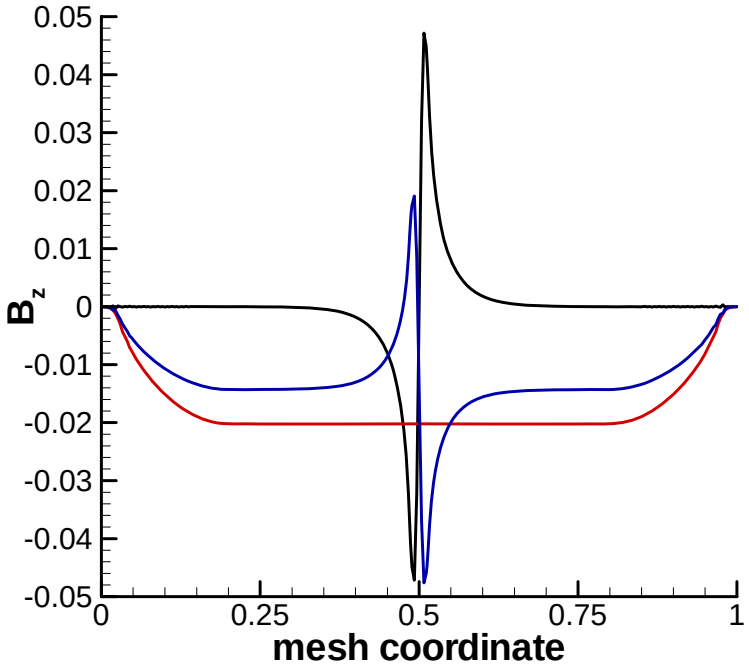

- An extremely packed mesh with ~50-100 high-order elements in x is required to resolve the tearing scale that is apparently smaller than $\sqrt{D_\eta/\gamma}$.
- Mesh uniformity becomes a problem packing elements to 100:1 aspect ratio.

The theory predicts that at small $\Delta'\delta$, two-fluid effects diminish with decreasing plasma-β.

Scanning plasma-β in a set of NIMROD tearing calculations with $\Delta' L$=0.277, S=9.3×10^4, and a/L=6 controls the magnitude of the two-fluid effect.

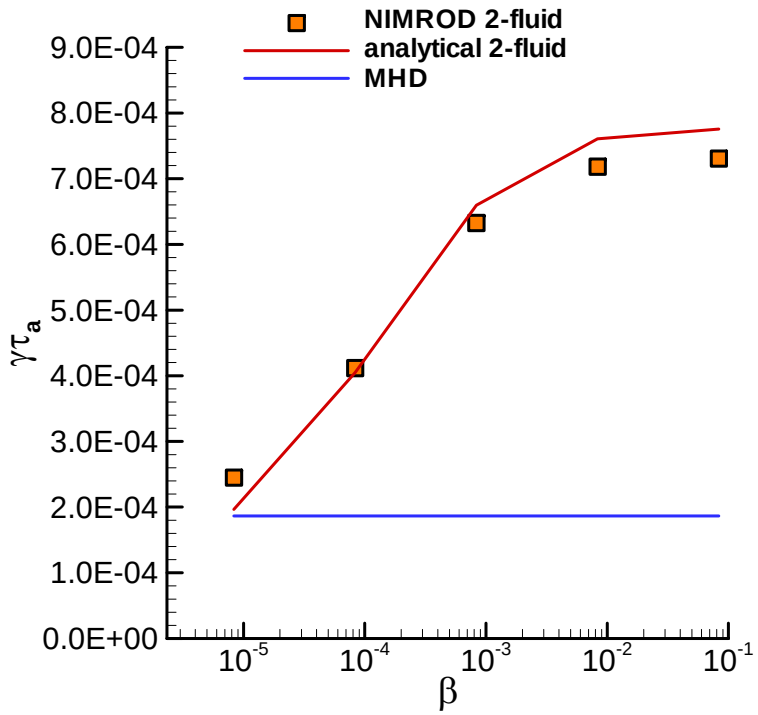

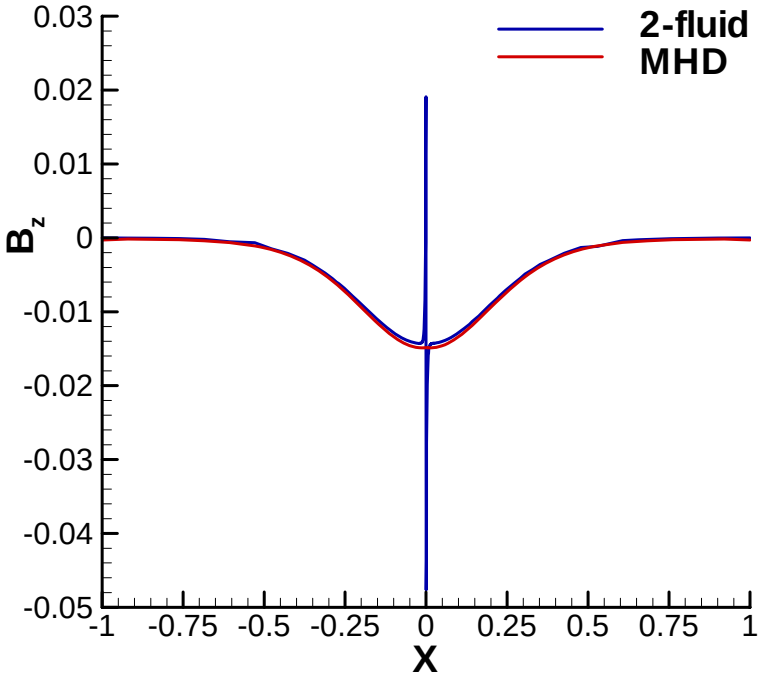

In the MHD limit, reconnection still occurs at a small scale, but the small-scale feature in B_z does not appear. [Here, the parameter set is from the previous page.]

The parallel electron stress is being added to the Ohm's law in NIMROD for neoclassical effects and to provide some smoothing of electron spatial scales.

- An implicit computation of the Braginskii fluid stress will be solved in the magnetic advance.
  - The fluid stress with arbitrary coefficient will allow direct modeling of Pfirsch-Schlüter regime bootstrap current.
  - The implicit operator will be used to stabilize nonlocal kinetic stress computations. [Held, PoP **11**, 2419 (2004)]
- The collisional form of the parallel stress is:

$$\Pi_e = -3\eta_0\left(\hat{\mathbf{b}}\cdot\nabla\mathbf{V}_e\cdot\hat{\mathbf{b}} - \frac{1}{3}\nabla\cdot\mathbf{V}_e\right)\left(\hat{\mathbf{b}}\hat{\mathbf{b}} - \frac{1}{3}\mathbf{I}\right)$$

with $\mathbf{V}_e = \mathbf{V} - \left(\frac{1}{1+Zm_e/m_i}\right)\frac{1}{ne}\mathbf{J} \cong \mathbf{V} - \frac{1}{ne}\mathbf{J}$

Implementation of parallel electron stress with basis functions having C^0 continuity requires an auxiliary field.

- With θ-centering in the time advance, we define $\nu \equiv \sqrt{3\Delta t \eta_0 \theta}/e\sqrt{\mu_0}$ and

$$f - \nu\left[\hat{\mathbf{b}}\cdot\nabla\left(\frac{\nabla\times\Delta\mathbf{B}}{n}\right)\cdot\hat{\mathbf{b}} - \frac{1}{3}\nabla\cdot\left(\frac{\nabla\times\Delta\mathbf{B}}{n}\right)\right] \equiv -\sqrt{\frac{3\eta_0\mu_0\Delta t}{\theta}}\left\{\hat{\mathbf{b}}\cdot\nabla\left(\mathbf{V} - \frac{1}{ne}\mathbf{J}^{\mathrm{n}}\right)\cdot\hat{\mathbf{b}} - \frac{1}{3}\nabla\cdot\left(\mathbf{V} - \frac{1}{ne}\mathbf{J}^{\mathrm{n}}\right)\right\}$$

- In weak form with $\mathbf{A}$ and g as the test fields, and dropping stress-related surface integrals, the magnetic advance is

$$\int_R d\mathbf{x}\left\{\mathbf{A}\cdot\Delta\mathbf{B} - \frac{\nabla\times\mathbf{A}}{n}\cdot\left[\hat{\mathbf{b}}\hat{\mathbf{b}}\cdot\nabla(\nu f) + \nu f\left(\hat{\mathbf{b}}\cdot\nabla\hat{\mathbf{b}} + \hat{\mathbf{b}}\nabla\cdot\hat{\mathbf{b}}\right) - \frac{1}{3}\nabla(\nu f)\right]\right\}$$

$$= -\Delta t\int_R d\mathbf{x}\,\mathbf{E}_{other}\cdot\nabla\times\mathbf{A} + \Delta t\int_{\partial R} d\mathbf{S}\cdot\mathbf{A}\times\mathbf{E}_{other}$$

$$\int_R d\mathbf{x}\left\{gf + \frac{\nabla\times\Delta\mathbf{B}}{n}\cdot\left[\hat{\mathbf{b}}\hat{\mathbf{b}}\cdot\nabla(g\nu) + g\nu\left(\hat{\mathbf{b}}\cdot\nabla\hat{\mathbf{b}} + \hat{\mathbf{b}}\nabla\cdot\hat{\mathbf{b}}\right) - \frac{1}{3}\nabla(g\nu)\right]\right\}$$

$$= \int_R d\mathbf{x}\left\{\frac{\mu_0 e}{\theta}\left(\mathbf{V} - \frac{1}{ne}\mathbf{J}^{\mathrm{n}}\right)\cdot\left[\hat{\mathbf{b}}\hat{\mathbf{b}}\cdot\nabla(g\nu) + g\nu\left(\hat{\mathbf{b}}\cdot\nabla\hat{\mathbf{b}} + \hat{\mathbf{b}}\nabla\cdot\hat{\mathbf{b}}\right) - \frac{1}{3}\nabla(g\nu)\right]\right\}$$

and for the curvature terms, $\hat{\mathbf{b}}\cdot\nabla\hat{\mathbf{b}} + \hat{\mathbf{b}}\nabla\cdot\hat{\mathbf{b}} = \frac{1}{B^2}\mathbf{B}\cdot\nabla\mathbf{B} - \frac{2}{B^4}\mathbf{B}[\mathbf{B}\cdot(\nabla\mathbf{B})\cdot\mathbf{B}]$

- For more information, see www.cptc.wisc.edu/sovinec_research/notes/e_viscosity2.pdf .

The simplest test of the parallel electron stress is the damping of whistler waves in a doubly periodic box.

- The NIMROD implementation presently has all of the linear terms for Π_e when η_0 is spatially uniform.
- Whistler tests for NIMROD have **k** and $\mathbf{B}_0$ in various orientations in the finite element plane and in the periodic (Fourier) coordinate.
- Results shown at right are obtained with an 8×8 mesh of bicubic elements and $\omega_r \Delta t \sim 0.1\text{-}0.2$.

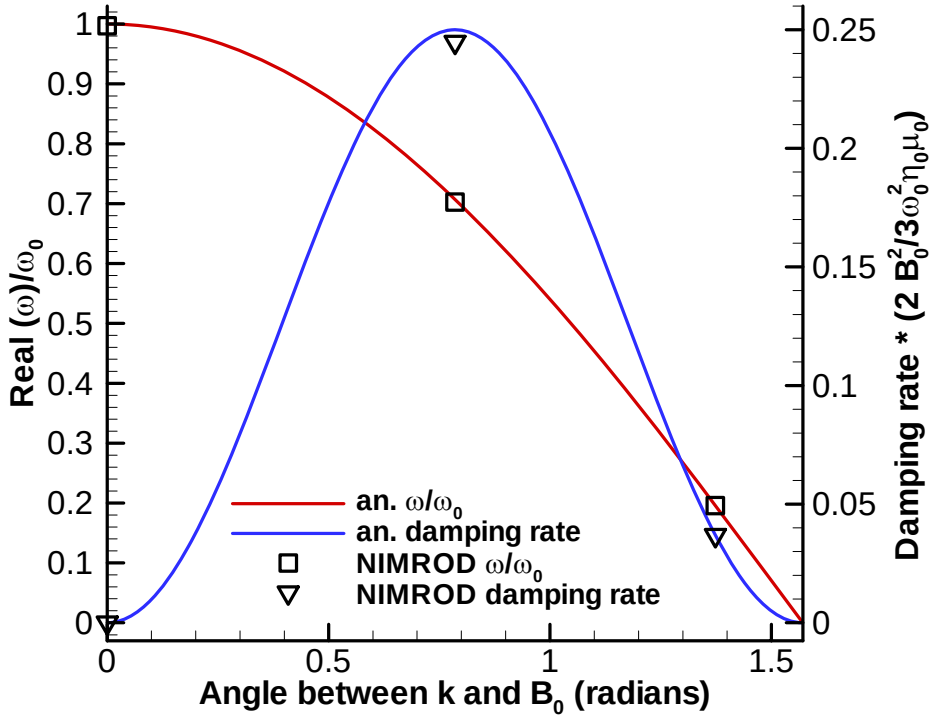

- The analytical dispersion relation is $\omega^2 + \left(\omega_0^2 \frac{k_\parallel^2}{k^2}\right)\left(i\frac{3\eta_0\mu_0 k_\perp^2}{B_0^2 k^2}\omega - 1\right) = 0\,,\ \omega_0^2 \equiv \Omega_i^2 d_i^4 k^4$

and for weak damping, $\omega_r^2 \cong \omega_0^2 \frac{k_\parallel^2}{k^2}$, $\omega_i \cong -\omega_0^2 \left(\frac{3\eta_0\mu_0 k_\parallel^2 k_\perp^2}{2B_0^2 k^4}\right)$

Our first results on reconnection with parallel electron viscosity show little effect on the growth rate and eigenfunction. This is expected due to the resonance condition together with the anisotropic nature of the stress.

- For the parameters of Case B in the table and a parallel damping rate of 8.0 τ_a^{-1} computed from $3\eta_0 k_y^4 B_{0_y}^2 \big/ n^2 e^2 \mu_0 B_0^2$ with η_0 set to 3×10^{-3} (MKS $\rightarrow$ $Jm^{-3}s^{-1}$), the growth rate of 5.12×10^{-3} τ_a^{-1} increases by less than 10% to 5.62×10^{-3} τ_a^{-1}.

- Near the tearing layer, $k_{||}^2$ is far smaller than at the wall, and the wall conditions have been used in the damping rate estimate of 8.0 τ_a^{-1}.

- There are only very slight changes in the eigenfunction just outside the tearing region.

- Computationally, a small level of thermal conduction has been used with the electron viscosity to avoid slowly growing noise.

- We expect that this term will have a greater effect in nonlinear calculations, where macroscopic changes in $\hat{\mathbf{b}}$ occur.

MRX Simulations

Full-geometry simulations of MRX with mesh packing around the reconnection site investigate coupling of tearing and global scales.

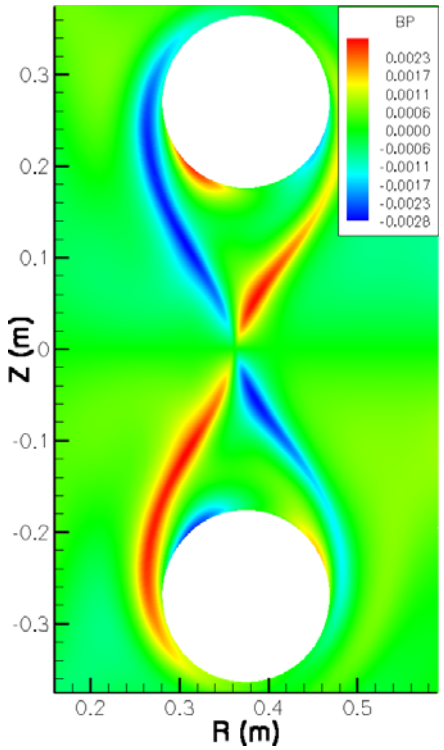

Out-of-plane component of magnetic field induced by Hall effect during simulated pull reconnection without guide field.

• Reconnection flows deplete mass from the smaller inboard volume, and the reconnecting region migrates inward.

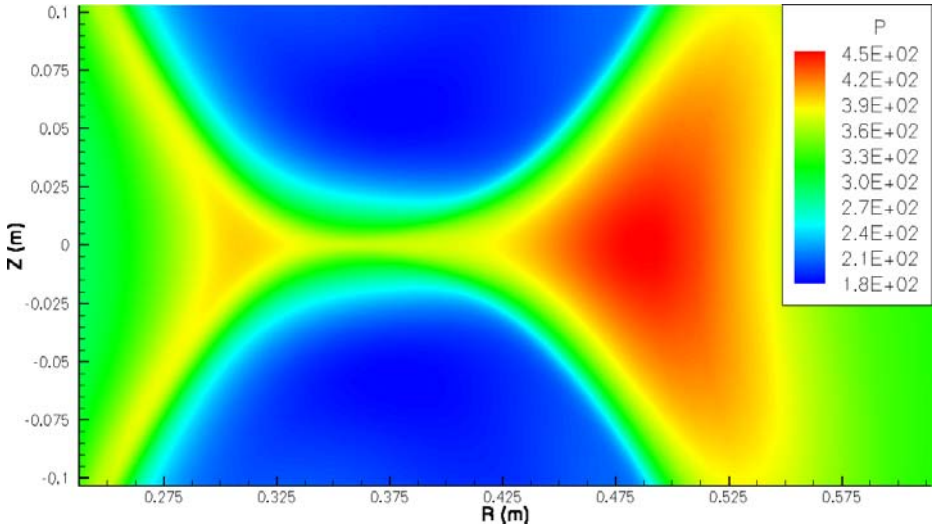

Pressure profile near the reconnection site from a simulated counter-helicity push configuration.

• Diamagnetic drift from the pressure build-up and out-of-plane field moves mass radially outward.

Conclusions

- The NIMROD code reproduces two-fluid tearing modes with large guide field over a wide range of stability parameter and plasma pressure.
- Nonlinearly, the Hall dynamo effect spreads along the island separatrix.
    - The nonlinear effect may explain the Hall dynamo profile measured in MST.
- The parallel electron stress contribution to Ohm's law is being developed.
    - Linear benchmark calculations on whistler waves verify expected damping rates.
    - It appears to have little effect on two-fluid tearing.
- This presentation will be posted on nimrodteam.org and www.cptc.wisc.edu/sovinec_research.